Chemical Conversion of Fischer–Tropsch Waxes and Plastic Waste Pyrolysis Condensate to Lubricating Oil and Potential Steam Cracker Feedstocks

Philipp Neuner [1,*], David Graf [1], Niklas Netsch [2], Michael Zeller [2], Tom-Carlo Herrmann [1], Dieter Stapf [2] and Reinhard Rauch [1]

1   Engler-Bunte-Institute (EBI), Karlsruhe Institute of Technology (KIT), 76131 Karlsruhe, Germany;
    david.graf@kit.edu (D.G.); therrmann.kit@gmail.com (T.-C.H.); reinhard.rauch@kit.edu (R.R.)
2   Institute for Technical Chemistry (ITC), Karlsruhe Institute of Technology (KIT),
    76344 Eggenstein-Leopoldshafen, Germany; niklas.netsch@kit.edu (N.N.); michael.zeller@kit.edu (M.Z.);
    dieter.stapf@kit.edu (D.S.)
*   Correspondence: philipp.neuner@kit.edu

Abstract: The global economy and its production chains must move away from petroleum-based products, to achieve this goal, alternative carbon feedstocks need to be established. One area of concern is sustainable production of synthetic lubricants. A lubricating oil can be described as a high boiling point (>340 °C) liquid with solidification at least below room temperature. Historically, many lubricants have been produced from petroleum waxes via solvent or catalytic dewaxing. In this study, catalytic dewaxing was applied to potential climate neutral feedstocks. One lubricant was produced via Fischer–Tropsch (FT) synthesis and the other lubricant resulted from low temperature pyrolysis of agricultural waste plastics. The waxes were chosen because they each represented a sustainable alternative towards petroleum, i.e., FT waxes are contrivable from biomass and CO_2 by means of gasification and Power-to-X technology. The pyrolysis of plastic is a promising process to complement existing recycling processes and to reduce environmental pollution. Changes in cloud point, viscosity, and yield were investigated. A bifunctional zeolite catalyst (SAPO-11) loaded with 0.3 wt% platinum was used. The plastic waste lubricants showed lower cloud points and increased temperature stability as compared with lubricants from FT waxes. There was a special focus on the composition of the naphtha, which accumulated during cracking. While the plastic waste produced higher amounts of naphtha, its composition was quite similar to those from FT waxes, with the notable exception of a higher naphthene content.

Keywords: lubricant production; waste pyrolysis; naphtha production; steam cracker

1. Introduction

Sustainability is a keystone to the future of global economics. The excessive burning of fossil resources is no longer a tolerable option for any long-term project. This is one of the reasons for research being conducted on renewable bio-based fuels. Many studies have focused on gasification of plant-based feedstock, and subsequently, used the resulting synthesis gas for reactions such as methanol-to-gasoline (MtG) [1] or Fischer–Tropsch (FT) synthesis [2]. While these work in principle, one of their major flaws is their economic viability, which results in fuels that are over current market prices. One possible solution may be the acquisition of high-value byproducts, such as lubricants from FT waxes, which usually achieve a much higher price than transportation fuels [3,4].

A similar problem exists regarding a different type of environmental concern, i.e., the increasing amount of plastic waste. Plastics are used in a manifold of applications and are almost irreplaceable in our modern economy. While the amount of plastics produced is steadily increasing, their recycling rates are only slowly catching up; 381 million tons of

new plastics were produced in 2015, while only 19.5% of the plastic waste was recycled that year. A large share of plastic waste is landfilled or discarded incorrectly causing environmental problems such as those associated with ocean plastics [5]. Energy recovery from plastic waste through incineration overcomes these issues but leads to fossil origin fixed carbons being emitted into the atmosphere, eventually contributing to climate change. In order to achieve a climate neutral circular economy of plastics, recycling processes for complex mixed wastes are needed. One such process is pyrolysis of plastic wastes, which may include a catalytic conversion step depending on the nature of the waste. Recent publications have focused mostly on the production of fuels from plastic wastes, which is an undesired utilization, as mentioned above [6,7]. One of the most significant issues for waste pyrolysis liquids is the utilization of its heavy phase (C_{21+}), a common approach is the application of severe hydrocracking, as was done by Choi et al. [8]. In their study, the focus was on the production of naphtha from polyolefins, which could then be reused as a steam cracker feedstock; however, the experiments were aimed at increasing the naphtha concentration in a liquid product, which led to the necessity of high conversion rates, and therefore, an extensive production of light gases. Another approach is retention and commercial exploitation of the heavy phase by turning it into lubrication oil via hydroisomerization. This requires less severe reaction conditions, which keeps the liquid yield higher. This process was patented in 2004 [9]. Nevertheless, the provided datasets in patents are limited.

Possible waste feedstocks for this process are polyolefins, which are the most used plastics globally. Currently, polyethylene (PE) is dominating. During thermal pyrolysis, PE degradates statistically resulting in a specifically high yield of high chain length aliphatics as compared with pyrolysis of other polymer types. These pyrolysis waxes (PW) can be hydroprocessed similar to FT waxes and turned into lubricants [10]. The production of lubricants from pyrolysis wastes could simultaneously solve many problems. An attractive application of pyrolysis liquids is the steam cracker. The production of olefins, which allow virgin and uncontaminated plastics to be remanufactured, is one of the most commonly discussed ways to reuse pyrolysis liquids as feedstocks. However, recently, it was stated by Kusenberg et al. [11] that untreated pyrolysis liquids based on waste plastics were unacceptable for industrial steam crackers and required an upgrading step such as hydrotreatment, which would also be required for any further hydrocracking or hydroisomerization step due to possible contaminants. Especially sulfur and nitrogen, which can act as a catalyst poison for the necessary noble metal and zeolite catalyst, need to be removed from pyrolysis liquids [12]. Hydroisomerization or cracking could provide a different application for the heavy residue fraction, which is not a preferred steam cracker feedstock, due to its high tendency to form coke. By combining hydrotreatment and hydroprocessing on polyolefin-based pyrolysis liquids, carbon recycling, and thus material utilization, can potentially be maximized.

The aim of this research was to determine the amount and quality of producible lubricant, naphtha, middle distillate, and hydrocarbon gas from a real waste plastic feed, which would allow a complete mass balance from plastic to end-product. Another focus was to provice detailed information about the naphtha composition, which is vital for possible steam cracker applications. A comparison with Fischer–Tropsch wax hydroprocessing was also performed, since FT products are known to produce high quality lubricants [13,14] and are easily applicable in a steam cracker [15,16].

2. Theoretical Background

2.1. Lubricant Production from Waxes

There are different methods of producing lubricants from waxes which are dependent on the desired lubricant properties and initial wax composition. Waxy behavior, which is characterized by high-temperature solidification, can usually be attributed to normal paraffin (n-paraffin) concentration in the feed. Normal paraffin must be removed (dewaxing) in order to lower the pour or cloud point and to achieve lubricity [17] and there are two

effective ways to do so. The first option is the physical separation of wax from the lubricant via solvent dewaxing. To achieve this, the wax is usually dissolved in a mixture of methyl ethyl ketone and toluene, and then cooled under agitation. This causes the n-paraffins to crystalize and precipitate which enables their removal via filtration [18,19]. The second route is the so-called catalytic dewaxing which utilizes a mesoporous catalyst to remove n-paraffins either via cracking or isomerization, depending on the chosen catalyst [20].

2.2. Hydroprocessing

The expression "hydroprocessing" serves as an umbrella term for multiple catalytic reactions under a hydrogen atmosphere. It can be used as a description for heteroatom removal (hydrotreating), removal of olefins (hydrofinishing), isomerization (hydroisomerization), or cracking (hydrocracking) of paraffinic feeds. In this study, it is used as a combination of hydroisomerization and hydrocracking, since these reactions proceed simultaneously. The mechanism is depicted in Figure 1 [21]. Due to the use of an acidic catalyst, a carbenium ion is formed on the surface, opening it up for cracking or isomerization at that position, with the latter being significantly faster. The carbenium ion is more stable on longer chains or highly isomerized chains, leading to a higher probability of irreversible cracking of the chain [22]. The high hydrogen pressure (up to 200 bars, depending on process and feed) is necessary to prevent catalyst coking [17].
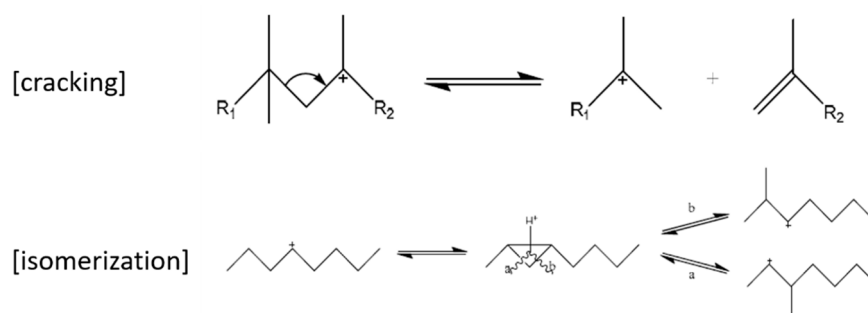

Figure 1. Mechanism of cracking and isomerization of n-paraffins [21].

2.3. Wax Production

There are many known wax sources available from multiple different origins, including natural sources such as beeswax or sugar cane wax. Alternatively, they can be of fossil origin such as petroleum waxes. Either way, they all consist of components of high molecular weight with long, straight chains in the form of n-paraffins, mono- and multi-ring naphtenes, aromatics, wax ethers, etc. [17,23,24]. Another product group are synthetic waxes, to which this work relates, and which are produced through a multitude of processes. Here, we are specially focused on Fischer–Tropsch waxes (FTW) and pyrolysis waxes (PW).

Synthetic waxes from FT synthesis are produced through the eponymous Fischer–Tropsch reaction (Equation (1)) [25]. Hydrogen and carbon monoxide react to produce a mixture of normal paraffins with broad chain length distribution, ranging from light gases, over naphtha and middle distillate to waxes. This results in a clean wax consisting almost entirely of n-paraffins, which are an excellent feed for dewaxing through isomerization. Due to the oil content being effectively zero, solvent dewaxing or removal of n-paraffins via cracking is not viable.

$$nCO + (2n + 1)H_2 \rightarrow C_nH_{2n+2} + nH_2O \tag{1}$$
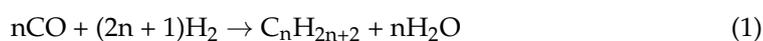
The second synthetic wax considered is retrieved from plastic pyrolysis. Pyrolysis is a high-temperature thermal decomposition process under inert atmosphere. By employing plastic waste as a pyrolysis feedstock, it can be used to break down high molecular weight (>>1000 g/mol) polymers into smaller chains, resulting in solid, gaseous, and vaporous products. After condensation of the vapors, pyrolysis condensate is obtained which can be

of liquid or waxy consistency, depending on the plastic feed and the process conditions. The pyrolysis gases and condensates are precious feedstocks for follow-up processes, making use of the carbon contained in the plastic. As compared with combustion, where the carbon in the plastic waste is emitted as carbon dioxide, pyrolysis is able to keep this carbon in cycle which makes the feed easier to handle by improving its fluidity at lower temperatures. This allows an easier application in follow-up processes. Polyethylene (PE) dominates polyolefincic wastes and tends to form a waxy brown condensate in pyrolysis processes at 450 °C to 500 °C. The liquids are described as pyrolysis wax (PW) which mainly consists of normal paraffins with various degrees of saturation. In that regard being similar to FTW, such pyrolysis condensates also provide an excellent feed for dewaxing operations, as has been shown by Miller et al. [10]. However, there are certain peculiarities regarding PW. Since plastic waste is not a pure substance, there are certain contaminations to be expected, which range from different varieties of plastics to heteroatom contaminations such as chloride, fluoride, bromine, or nitrogen, which can severely harm the hydroprocessing catalysts. In the case of chlorine, it can even damage the plant periphery. Due to the disposal of composite materials in regular waste, there is also the possibility of metal contamination.

The issues are well known and have lead to many publicized works on virgin plastics. The aim of this research was to examine lubricant production from a real waste plastic feedstock, to determine potential yields and to examine the purification effort.

3. Materials and Methods

3.1. Pyrolysis Reactor

The pyrolysis experiments were conducted using a pilot scale pyrolysis screw reactor at the ITC (Figure 2). The system is described in detail by Zeller et al. [26]. There are two hoppers with screw feeders, one for the plastic waste and the other for additives. During continuous operation, the plastic throughput is approximately 1 kg/h with 4 kg/h of quartz sand added to facilitate heat and mass transfer. The reactor is continuously flushed with nitrogen. The pyrolysis gases and vapors are extracted from the reactor via filter elements in the free board and fed to the condensation unit, where condensable products and permanent gases are separated in two stages at 60 °C and 5 °C. The condensable products are collected in glass bottles. Solid pyrolysis products are held back from pyrolysis gas and vapors prior to condensation using a hot gas filtration system and are collected in a vessel at the end of the screw reactor. To calculate product yields, a predetermined amount of plastics was fed into the reactor. Afterwards, the resulting liquids and solids were weighted. The gaseous products were transferred to an online gas analysis system and subsequently fed to a flare. Not determinable mass iwas considered to be balance loss. Two independent test runs were carried out to ensure the reproducibility of the results. For each test run, a 7.5 kg feedstock mixture of LDPE film and lime was used to which approximately 0.2 kg/h of slaked lime ($Ca(OH)_2$) was added as a chlorine scavenger. A steady-state operation was reached after approximatelhy 45 min.
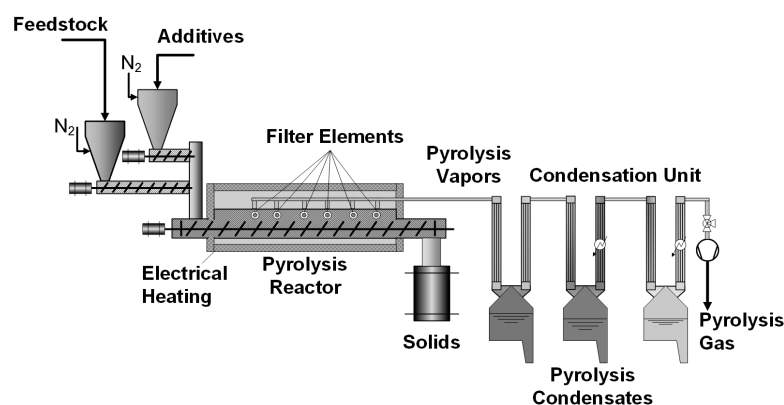

Figure 2. Pyrolysis reactor at the Institute for Technical Chemistry (ITC) at KIT [26].

3.2. Hydroprocessing Reactor

The hydrogenation and hydroprocessing experiments were conducted on a three phase fixed-bed reactor located at the Engler-Bunte-Institute in Karlsruhe. It consists of a heatable piston pump (HPD Pump Multitherm 200 model 3351, BISCHOFF Analysentechnik u. -geräte GmbH, 71229 Leonberg, Germany), which allows processing of waxy feeds in the range of 0.01–5.00 mL/min. Hydrogen and argon is supplied by mass flow controllers (Bronkhorst El-Flow, Wagner Mess- und Regeltechnik GmbH, 63073 Offenbach am Main, Germany). The reactor itself consists of a stainless steel tube with an inner diameter of 14.9 mm. For temperature measurements inside the fixed bed, a 1/8 inch tube was inserted in the center. A detailed description can be found in recent publications [27]. A schematic depiction is shown in Figure 3. The reactor was operated continuously, with the liquid sample for each measurement point being collected all at once at the liquid separation vessels. Liquid educt consumption was determined via load cell, which was used as the basis for subsequent product yields. The liquid products were weighted after separation. The gas flow was determined via GC (Section 3.5.1).
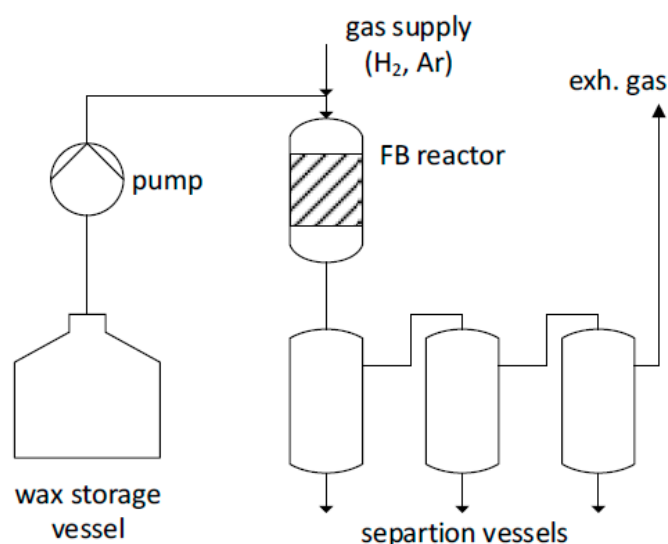
Figure 3. Three phase fixed-bed reactor at the Engler-Bunte-Institute (EBI) at KIT [27].

3.3. Feedstocks

Two different materials were used as feedstock basis for the investigations. The first feedstock was a hydrogenated and slightly isomerized commercial Fischer–Tropsch wax from Sasol. It had a high n-paraffin content, and therefore, was completely free of pollutants such as halogens or oxygenates, which made it an optimal feed for hydroprocessing operations. The second feedstock was a self-generated plastic waste-based pyrolysis oil. Hereto, waste agricultural films were used as pyrolysis feedstock. It consists mainly of low-density polyethylene (LDPE) with small fractions of other polyolefins, hence, producing a waxy effluent after pyrolysis. However, contamination of the pyrolysis condensate was expected due to contact of the plastic with organic matter during usage and the addition of dyes and performance enhancers to the plastic such as UV stabilizers. These impurities required a preceding hydrogenation step, which was not done for the FT waxes. The feed wax compositions are shown in Figure 4. Due to the difficulties associated with analyzing pyrolysis wax, only the carbon range was determined.
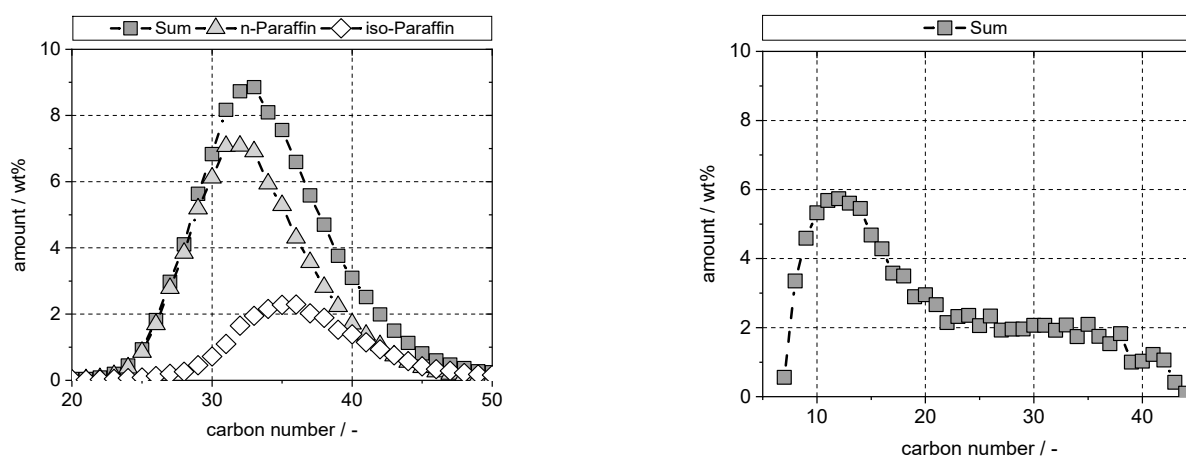
Figure 4. Chain length distribution of the Fischer–Tropsch wax (**left**) and pyrolysis wax (**right**) via simulated distillation.

3.4. Catalysts

For the experimental procedures, two commercially available catalysts were used. The hydroprocessing experiments were conducted on a SAPO-11 (AEL structure) zeolite with 0.3 wt% platinum loading. It was chosen for its low acidity and narrow pore structure, which leads to high isomerization selectivity [28]. Isomerization of the heavier molecules was necessary to produce paraffinic lubricant. The pyrolysis wax contained a high amount of residual sulfur compounds. Since sulfur is a potent catalyst poison for noble metal catalysts, it had to be removed via hydrogenation [29]. A commercial cobalt-molybdenum (CoMo) catalyst was chosen, which is a widely used metal combination for desulfuriza-tion operations [30,31]. The details are listed in Table 1. For preparation, the catalysts were ground down and sieved to a particle size of 100–200 μm. They were filled into the reactor and oxidized at 450 °C for 6 h, or until no temperature peak was detectable anymore. Afterwards, they were reduced under hydrogen atmosphere at 450 °C for 72 h (CoMo/Al$_2$O$_3$) and at 400 °C for at least 3 h (Pt/SAPO-11). After regeneration of the SAPO catalyst, the sample of the initial 24 h of runtime were discarded due to coke residue being flushed out after oxidization and to avoid a spike in the initial catalyst activity. To avoid the introduction of unnecessary amounts of sulfur into the reactor, we chose not to sulfide the hydrotreatment catalyst.

Table 1. Catalysts used during the experimental procedures.

Catalyst	Metal Loading (wt%)	Catalyst Mass (g)	Catalyst Volume (mL)
Pt/SAPO-11	0.3 wt%	20.005	22.10
CoMo/Al$_2$O$_3$	15.5 wt%	39.570	48.77

3.5. Utilized Analytical Instruments

3.5.1. Gas Phase

The conducted experiments resulted in two different gas streams. While pyrolyzing the plastics and condensing the vapors, permanent gases left the condensation unit. The so-called pyrolysis gases were not analyzed for this work. The second gas effluent was discharged during the hydroprocessing experiments. It was constantly analyzed via online GC measurements (Agilent 7890A GC, Agilent Technologies Germany GmbH & Co., KG, 76337 Waldbronn, Germany). Two detectors were used (FID and TCD). A small amount of argon (10–15 mL/min) was added to the feed gas, which was used to calculate the hydrocarbon concentration in the gas stream.

3.5.2. Naphtha and Middle Distillate

The light naphtha fractions were analyzed via a PAC Reformulyzer M4. With this method, a detailed description of their exact composition was possible. The amount of n-paraffins, isoparaffins, naphtenes, aromatics, olefins, and cyclic olefins could be given for each individual carbon chain length, up to C_{12}. No significant amount of oxygenates could be measured in the pyrolysis samples. The chain length distributions in the liquid phase were analyzed using simulated distillation (Nexis GC-2030, Shimadzu Germany GmbH, 47269 Duisburg, Germany). The degree of saturation in the middle distillates was determined via low-field ^{1}H-NMR (Spinsolve Multi X Ultra 80 MHz, Magritek, 52068 Aachen, Germany).

3.5.3. Lubricants

Cloud point determination was done using differential scanning calorimetry (DSC 214 Polyma, Netzsch-Gerätebau GmbH, 95100 Selb, Germany). For each measurement, 10 mg of the sample was weighted in a sealable aluminum crucible. The sample was kept at a constant temperature for 5 min, afterwards it was cooled down to 10 K/min. At cloud point temperature, the signal peaked. This peak indicated the start of crystallization at the intersection of its tangents. An example measurement of a commercial paraffin oil is shown in Figure 5.
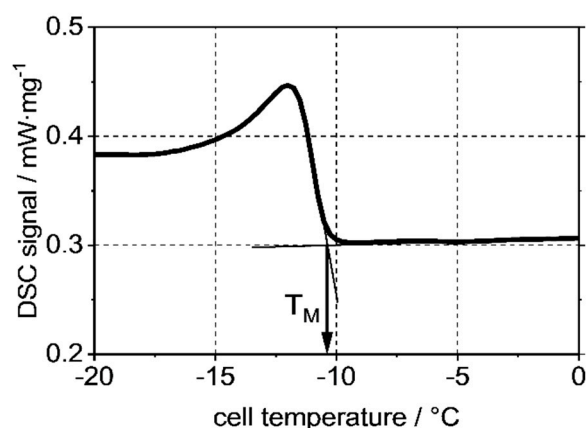
Figure 5. DSC signal for a commercial paraffin oil at cloud point temperature [27].

The measured temperature (T_M) needed to be subjected to calibration functions, which were determined by measurements of solidification temperatures of pure substances. To validate the accuracy of this method, two cloud point reference samples (determined according to ASTM D 2500 [32]) were acquired, analyzed, and compared. This comparison resulted in a slight deviation between the different methods (Table 2). However, this discrepancy was within the standard deviation given by the ASTM method and within the scope of accuracy of DSC measurements described in other publications [33].

Table 2. Comparison of cloud point values obtained via ASTM and DSC method.

	CP (ASTM D 2500)	CP (DSC)
Sample 1	$+7.7\,°C \pm 0.6\,°C$	$+8.29\,°C$
Sample 2	$-21.0\,°C \pm 2\,°C$	$-19.09\,°C$

For viscosity measurement, a plate rheometer (MCR 302e, Anton Paar Germany GmbH, 73760 Ostfildern-Scharnhausen, Germany) was used at a constant sheer rate of $50\,s^{-1}$ and a 50 mm plate, for at least 10 min. The density was determined by oscillating tube measurements (DMA 4200, Anton Paar Germany GmbH, 73760 Ostfildern-Scharnhausen, Germany). The infrared measurements were conducted on a Bruker Vertex 70 FT-IR Spectrometer.

4. Results

4.1. Pyrolysis of Plastic Feedstock

During pyrolysis of the feedstock described in the previous section, almost identical results for each test run were obtained regarding the mass and energy balances. By averaging the individual balances, a weight0related yield of organic condensate of approximately 64.4 wt% was determined. As byproduct, 35.0 wt% pyrolysis gas was generated. Solid residue such as coke was observed only to a negligible extent. The balance loss accounted for 0.6 wt%. A minimum energy demand was measured. It involved heating the feedstock mixture to reactor temperature, melting the thermoplastic components, the endothermic pyrolysis reaction, evaporation of the resulting pyrolysis products, and other possible endothermic processes in connection with the feedstock, such as impurity scavenging reactions by lime or other reactions of the additive. This feed-related minimum energy demand was 2.21 MJ/kg.

4.2. Hydroprocessing of the Fischer–Tropsch Wax and Pyrolysis Wax

The pyrolysis wax had to undergo severe hydrogenation (Hyd.) before further hydroprocessing (HP) steps could be performed, due to the excessive amount of residual sulfur in the pyrolysis wax sample. Therefore, two consecutive hydrodesulfurization steps with increasing pressure, temperature, and flow rate were applied. The two-step approach was necessary due to the strongly exothermic behavior of the pyrolysis wax and the inability to cool the reactor, which could have led to temperature spikes and increased cracking reactions. The initial hydrogenation allowed an increased flow in the second step, due to its effective isothermic behavior. However, this two-step approach might not be necessary with an appropriate setup. The pyrolysis wax exhibited extremely corrosive behavior towards the HPLC pump, which required multiple stops, especially during the first hydrogenation step. Over the maintenance time, the catalyst was kept at reaction pressure and hydrogen atmosphere, which resulted in partial regeneration. Therefore, it was not possible to reliably investigate sulfur deactivation. Afterwards the hydrogenated and sulfur-free wax was subjected to independent hydroprocessing over SAPO-11 catalyst at different reactor temperatures. The Fischer–Tropsch wax did not need additional hydrogenation and was directly used for hydroprocessing. The complete process parameters are listed in Table 3.

Table 3. Process parameters for hydroprocessing experiments in the fixed-bed reactor. Gas flows are given at laboratory conditions.

	T (°C)	P (Bar)	$\dot{V}_{wax}$ (mL/min)	$\dot{V}_{H2}$ (mL/min)	$\dot{V}_{Ar}$ (mL/min)	Applied Feeds
Hyd. 1	280	100	0.56	1100	10	PW
Hyd. 2	360	130	1.12	1100	10	PW
HP 350 °C	350	100	0.42	825	15	FTW/PW
HP 370 °C	370	100	0.42	825	15	FTW/PW
HP 390 °C	390	100	0.42	825	15	FTW/PW

4.3. Distillation and Product Yields

The products were separated via distillation after each step to investigate changes in composition and product yields. The chosen boiling ranges were defined as; naphtha <170 °C, middle distillate 170 °C–340 °C, and heavy residue >340 °C. The sulfur removal through hydrogenation was not complete after the first step, only removing ~68%. After the second step, its amount fell below the detection limit. It could, therefore, be treated as sulfur-free (Table 4). The amount of nitrogen was measured below 0.2 wt% for all samples, which was outside the calibration range, therefore, no trends could be given.

Table 4. Sulfur content of pyrolysis wax before and after hydrotreatment.

	Educt (mg/kg)	Hyd. 1 (mg/kg)	Hyd. 2 (mg/kg)
Sulfur concentration	726 ± 13	270 ± 6	<30

The overall product composition is depicted in Figure 6. The hydrogenation steps barely change the composition, only after the second step, a slight decrease in heavy residue can be detected, which is due to cracking reactions during hydrogenation. The loss of naphtha after Hyd. 2 is most likely due to the higher distillation loss that occurred in this case. However, the hydroprocessing reactions had a pronounced effect on product composition, with the amount of naphtha and light gases increasing rapidly with reaction temperature, while the amount of heavy residue and middle distillate was decreasing. It is interesting to note that the sum of naphtha and middle distillate stayed around 60 wt% of the feed regardless of the applied upgrading step.
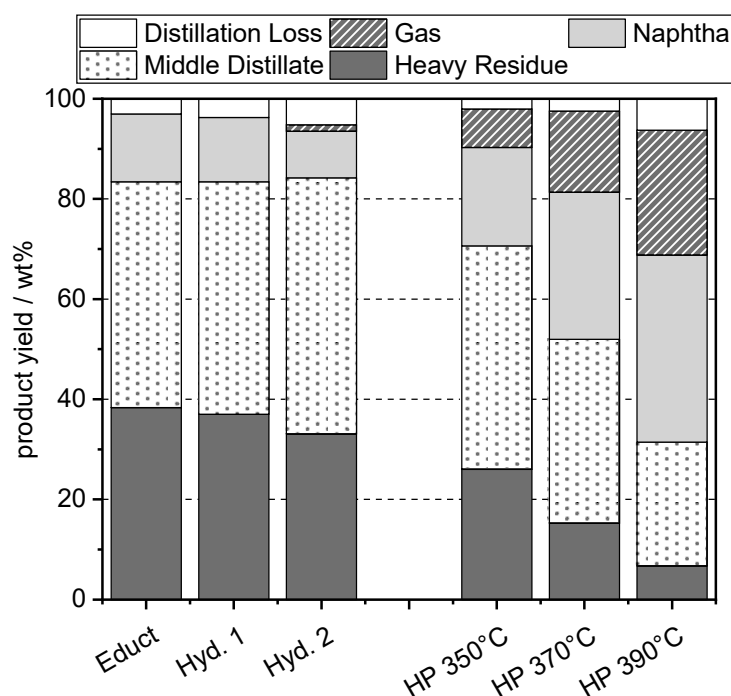
Figure 6. Product yield of pyrolysis wax hydroprocessing as listed in Table 2.

The yield composition of the pyrolysis wax hydroprocessing was compared to the those of the FT wax at identical process parameters. The results are depicted in Figure 7. While the trends of increasing naphtha and gas yields while simultaneously decreasing the amount of middle distillate and heavy residue stay identical, the overall composition is different. The pyrolysis samples show constantly higher amounts of fuel fractions than those of their FT counterparts. The produced gas phase for PW is also increasing significantly faster with temperature. These effects can be attributed to the higher amount of short chain molecules formed in the pyrolysis process. Interestingly, the amount of liquid product lost into the gas phase is rather similar for lower reaction temperatures, despite the shorter chains in the PW samples. This indicates a higher cracking preference of long chains as compared with shorter chain molecules, which are only removed, once the temperature is high enough. This indicates that a removal of the naphtha phase before hydroprocessing might not significantly improve the overall liquid yield at moderate temperatures.
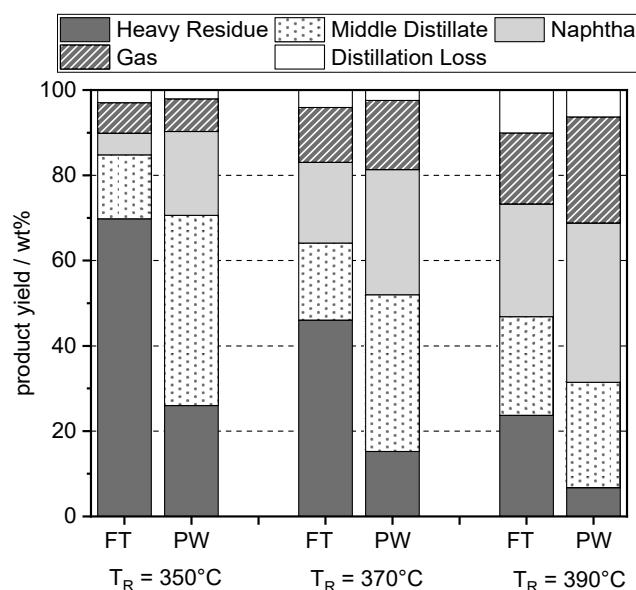
Figure 7. Comparison of product yields after HP of FTW and PW.

4.4. Approximate Product Yields

As stated in the beginning, one of the goals of this study was to determine the possible yield of lubricants and their byproducts from a real plastic waste feed. An exemplary flow diagram for the reaction parameters HP 370 °C is shown in Figure 8 and a detailed list of all parameters is presented in Appendix A. Due to the difficulties associated with accurately measuring hydrogen consumption in the process, the amount of hydrogen necessary was calculated via elemental analysis of the liquid wax before and after hydrogenation via comparison of the difference in the H/C ratios. This ratio had to be raised from 1.96 in the educt wax to 2.03 after Hyd. 2, indicating partial hydrogenation. The amount of hydrogen necessary for the HP experiments was determined using the change in chain lengths of the products, assuming them to be fully hydrogenated paraffins (C_nH_{2n+2}). Impurities were not considered. With those assumptions, the overall amount of hydrogen necessary was determined to be 13.2 $kg_{H2}/t_{Plastic}$ or 305.6 $L_{H2,STP}/L_{Pyrolysis\ wax}$. The ratio of hydrogen needed for each step can shift, depending on the severity of the initial hydrogenation step. For the case of HP 370 °C, the potential yield of lubricants is rather low, with approximately 98.1 $kg_{Lubricant}/t_{Plastic}$. The largest product fraction is light gases, with an overall gain of 453.0 $kg_{Gases}/t_{Plastic}$. The yield of fuel is slightly lower with 425.7 $kg_{Liquid\ fuels}/t_{Plastic}$.
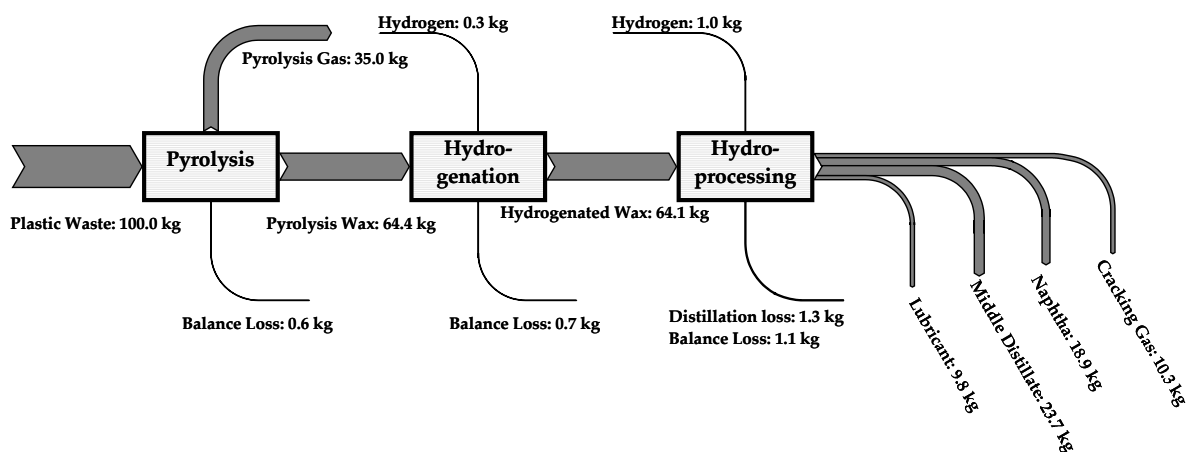
Figure 8. Flow diagram of product yield for catalytic treatment of agricultural films for conditions of HP 370 °C.

4.5. Lubricant Properties

After the PW hydroprocessing experiments and separation, the lubricant properties were investigated and compared to its FT counterparts. The PW samples generally showed a lower cloud point, varying between 5 °C and 20 °C deviation from the those of FT wax (Figure 9). If the values are plotted into a CP/yield graph, the overall yield of PW lubricant is worse than for FT waxes. This is due to the lower amount of heavy residue in the PW feed (Figure 10). If the results are adjusted to the heavy residue content, it can be seen, that the cloud points for PW lubricants are lower at identical yield as compared with FT lubricants.
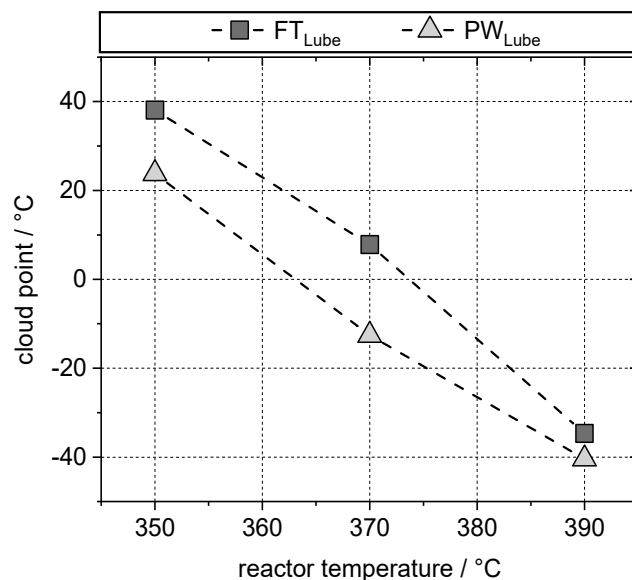
Figure 9. Cloud points of FT and PW lubricant over reaction temperatures at p = 100 bar, V_{wax} = 0.42 mL/min.
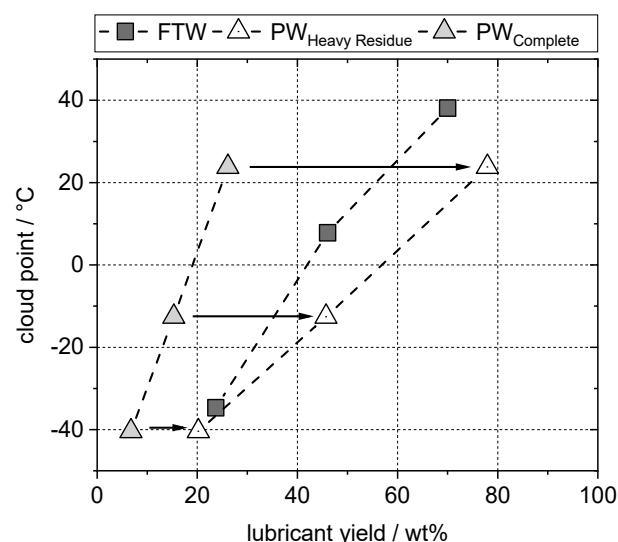
Figure 10. CP/yield graph of FT and PW lubricant samples. The grey triangles depict the de facto lubricant yield from pyrolysis wax, while the white triangles symbolize the yield in relation to the amount of heavy residue after the hydrogenation experiments (33.5 wt% in Hyd. 2).

A comparison of the viscosities was performed at 100 °C to avoid the influence of crystallization at lower temperatures. The dynamic viscosity is in the range of approximately 2.5–4.5 mPas, while the kinematic viscosity is slightly higher at around 3.2–5.6 mm^2/s (Figure 11a,b). The measured viscosity decreases with rising reactor temperature. However,

the biggest decay is visible between 370 °C and 390 °C, when cracking reactions take over and the higher chain length molecules are removed from the product. Between 350 °C and 370 °C, the changes are only marginal. In the case of PW_{Lube}, the viscosity can be seen as constant in this area. Individual data points are given in Appendix C. To determine the possible use cases for the lubricants, the viscosity index (VI) was determined. This index is used to describe the temperature stability of lubricating agents. Since waxy n-paraffins having high VIs, the results were plotted against the lubricant cloud points to compare their cold flow properties with temperature stability. The results are depicted in Figure 11c. It shows that, in general, the lubricants from PW exhibit better temperature stability than the FT lubricants. This is most likely due to the immense spectra of possible byproducts originating during pyrolysis. However, to prove this assessment, further investigations, especially regarding lubricant composition, need to be done. The overall range of VI was between 120 and 200, which would classify the lubricants as multigrade oil, which could have multiple possible applications. Nevertheless, due its low viscosity, it is not suitable for most motor oil uses. It needs to be stated that any final lubricant application would need some form of additives or refinement steps, therefore, any produced lubricant can only be treated as a so-called "base-stock".

(a)

(b)

(c)
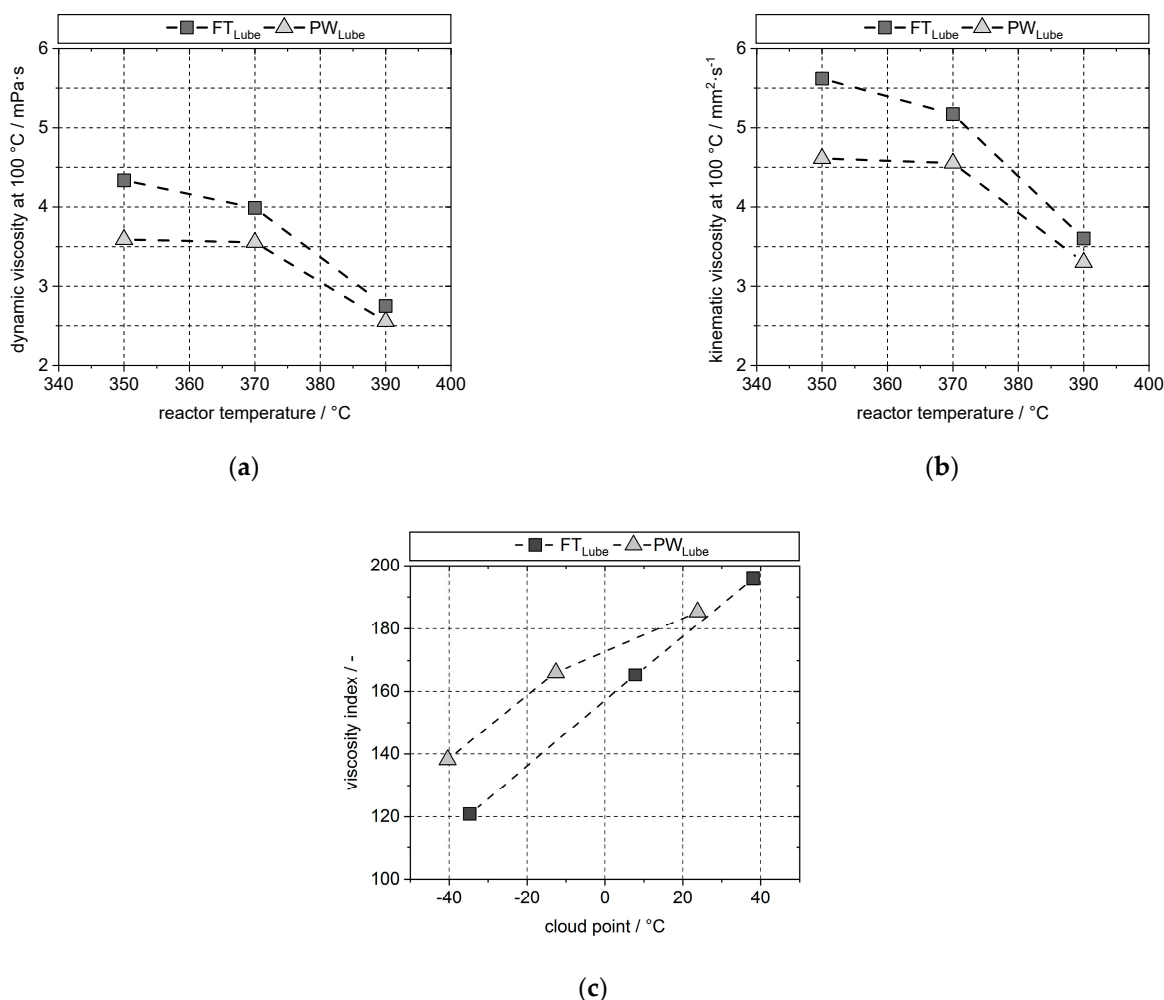
Figure 11. Dynamic (**a**) and kinematic (**b**) viscosity for lubricants/waxes at different reactor temperatures and viscosity index values of FT and PW lubricants plotted against their individual cloud points (**c**).

Another issue is to clarify whether it is feasible for real plastic feedstock to be converted into pharmaceutical grade white oil. However, in this study, it was not possible to prepare

a finished product due to time and material constraints. The amount of lubricant produced did not exceed 250 mL for any given set of reaction parameters. Therefore, it was not feasible to purify the low amount of lubricant with the available fixed-bed reactor. Nevertheless, it was still possible to clarify if the produced lube could be treated as a so-called "base-stock" for pharmaceutical white oil by confirming its identity as paraffinic. The European pharmacopeia [34] entails multiple tests for "paraffinum liquidum", however, most of the requirements are solvable with postprocessing steps, which are the test for acidic/alkaline components, and the presence of polyaromatic hydrocarbons (PAH) and general impurities. These can all be solved with a full hydrogenation, which is required to achieve a clear color. The other tests are density, viscosity, and cloud point. The cloud point can be reduced below the required 0 °C, as shown in the figures above. Density and viscosity are mainly determined by the average chain length of the lubricant [35], and therefore can, if necessary, be adjusted via distillation temperature. This leaves only one crucial test left, which is validation of identity via IR spectroscopy. To investigate, whether this product was suitable for such an application, the spectrograms for the PW lubricants were recorded and compared to a commercially available pharmaceutical white oil. The results are depicted in Figure 12. It is notable that there are no significant changes in the absorbance spectra regardless of the process temperature. There are also no interference peaks. Therefore, it can be assumed that all produced lubricants from this specific plastic feed would be applicable as pharmaceutical base stock if a hydrofinishing step were to be applied.
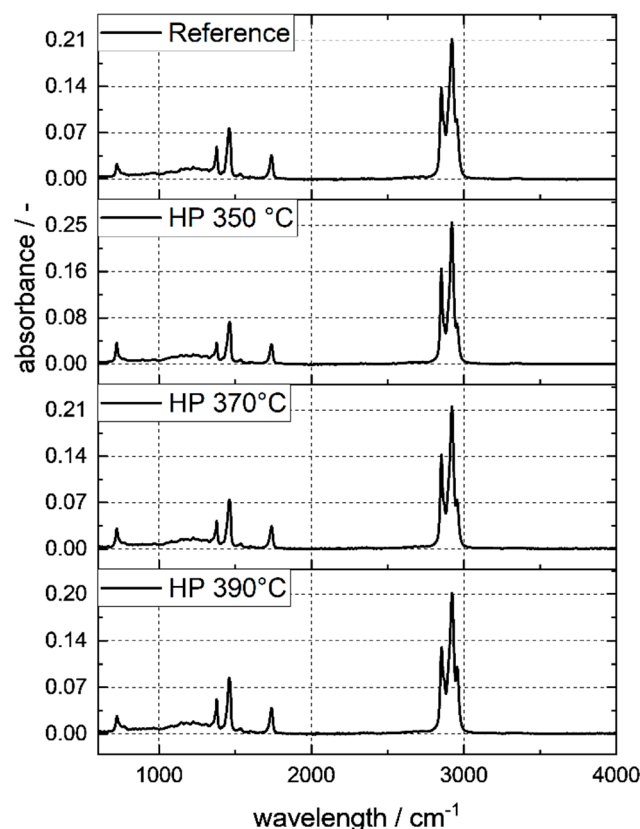
Figure 12. FTIR spectrograms of PW lubricants and pharmaceutical white oil (Reference: Paraffinum liquidum PH.EUR. 9.5, Caesar & Loretz GmbH, 40721 Hilden, Germany).

4.6. Naphtha Composition

Furthermore, to determine the possible uses for the naphtha fractions, it is pivotal to know their exact composition. Therefore, the light naphtha was analyzed using a Reformulyzer M4, separating them into their substance groups such as aromatics, olefins, n-/iso-paraffins, and naphthenes. The results are depicted in Figure 13. The educt naphtha

shows a significant amount of unsaturated products, consisting of a mixture of cyclic and linear olefins and a high amount of aromatics. After hydrogenation, almost all of the olefins are converted, however, the amount of aromatics changes comparably little. Even after the second hydrogenation step, the amount of aromatics stays the same, even though the olefins are effectively removed. The share of naphthenes increases with each hydrogenation step, while n-/iso- paraffins stay almost identical, which is due to the amount of aromatics and cyclic olefins being saturated during the process. An exact list of every component divided by chain length is shown in Appendix B. The individual hydroprocessing steps show a significant increase in isoparaffins with a simultaneous decrease in n-paraffins. However, the residual amount of aromatics is effectively reduced to zero, indicating the necessity of noble metal catalysts, if the removal of aromatic compounds is required. As compared with the cracking of FTW, the naphtha compositions are almost identical, except for a constantly higher amount of naphthenes (Figure 14).
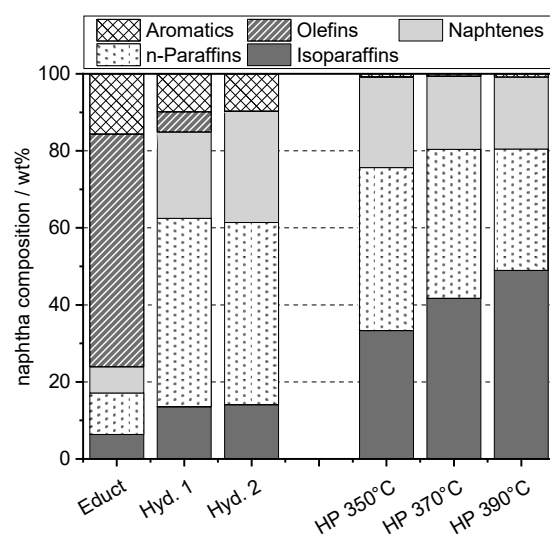
Figure 13. Naphtha composition after the subsequent hydrogenation steps and individual hydroprocessing at different temperatures.
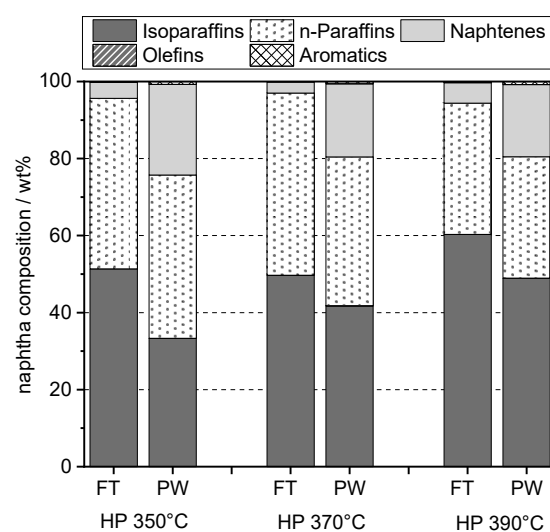
Figure 14. Comparison of naphtha compositions after HP of FTW and PW.

As mentioned above, one main utilization of naphtha from plastic waste is its decomposition via steam cracker to prepare high value olefins such as ethylene or propylene to produce polymers once again. For steam cracking purposes, the composition of its

naphtha feed is of utmost importance. The desired feed composition consists mainly of n-paraffins since they result in higher ethylene yield. Isoparaffins and naphtenes generally see slightly lower yields in that regard [36]. Unsaturated compounds are the least desirable for steam crackers because they tend to produce high amounts of unusable heavy residue and coke [37]. With these effects in mind, the overall amount of each component in regards to the deployed mass of pyrolysis wax is plotted in Figure 15.
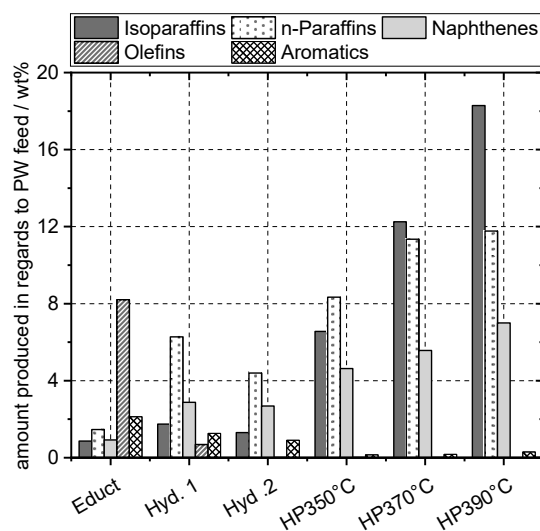
Figure 15. Produced substance groups in the naphtha phase in relation to PW feed.

It can be seen that any product before hydroprocessing is not desirable due to its low overall yield and the high content of olefins and aromatics. The yield of desirable n-paraffins increases with reactor temperature, but plateaus at 370 °C, while the isoparaffin and naphthene yield continues to rise afterwards. Coincidently, the set point at HP 370 °C also produced the most suitable lubricant base stock in regard to yield and potential applications. This indicates a potential optimum around the 370 °C mark for the SAPO-11 catalyst for co-production of lubricant and steam cracker feed.

4.7. Middle Distillate Composition

For the middle distillates, effectively, all the statements made above are confirmed as well. If the resulting fuel fractions from waste plastics cannot be used in combustion engines legally, steam cracking remains an attractive option. Certain steam crackers can handle heavier feedstocks [38]. However, the amount of aromatics and olefins needs to be low to prevent soot formation, as previously explained. Due to the Reformulyzer being unable to handle products with a boiling range higher than 200 °C, the middle distillates were analyzed using ^{1}H-NMR; these analyses did not represent an absolute amount, and therefore, could only be used comparatively. The results are depicted in Figure 16 and Table 5. Aliphatic saturated hydrocarbons (0.5–2.8 ppm) dominate the middle distillate fraction, while the middle distillate educt shows a significant amount of olefins (4.5–6.3 ppm), which are visibly reduced during the hydrogenation steps. However, to remove as many aromatics (6.3–8.7 ppm) as possible, noble metal catalyzed hydroprocessing experiments are necessary, since they are barely affected by the initial hydrogenations.
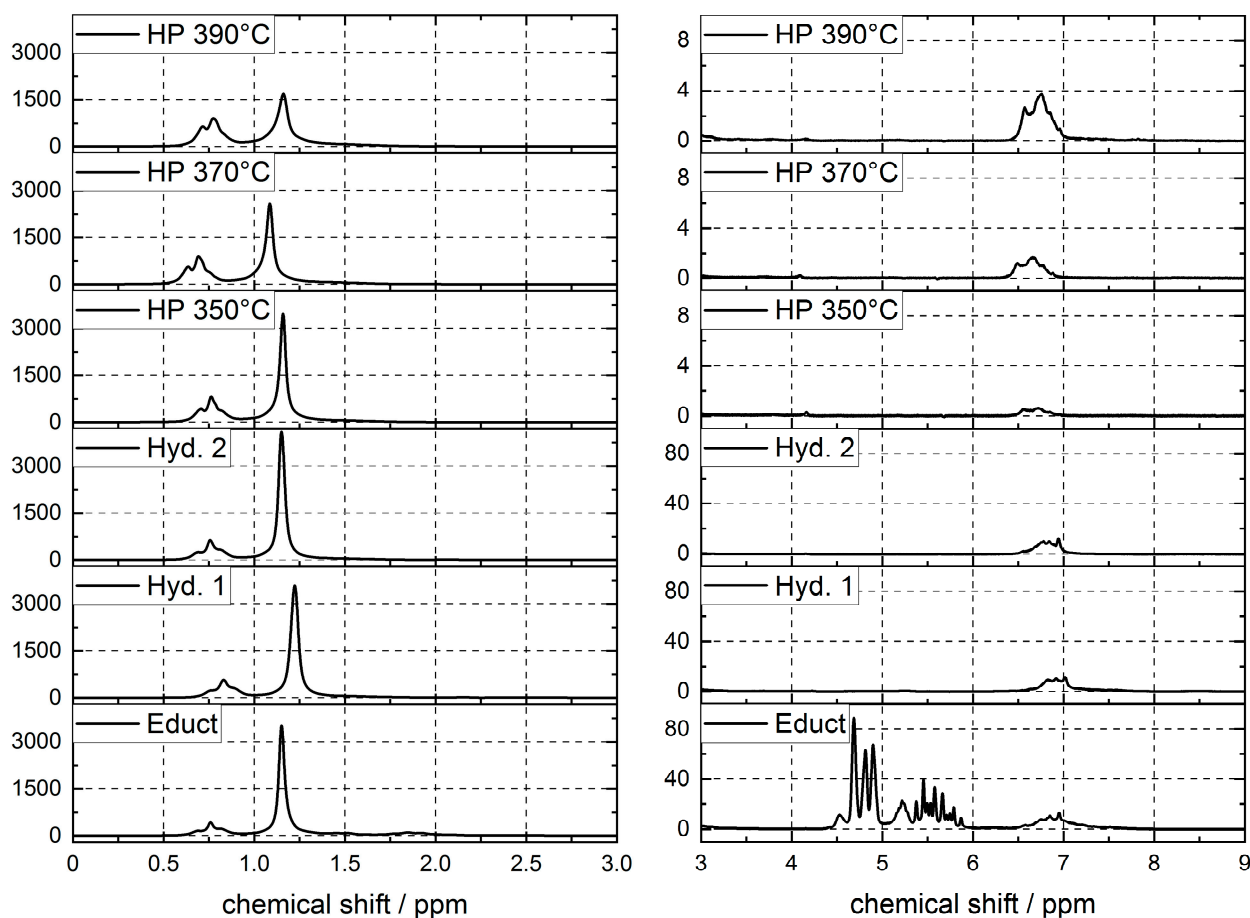
Figure 16. ^{1}H-NMR spectra of PW middle distillates after hydrogenation and hydroprocessing (note the difference in *y*-axis scaling for the HP experiments on the right side).

Table 5. Composition of pyrolysis wax middle distillates from ^{1}H-NMR after hydroprocessing, given in area percentage.

	Olefins	Aromatics	Aliphatic Comp.	CH3	CH2	CH	Other
	4.5–6.3 ppm	6.3–8.7 ppm	0.5–2.8 ppm	0.5–1.2 ppm	1.2–1.5 ppm	1.5–2.0 ppm	2.0–2.8 ppm
Educt	7.1	1.5	91.1	15.7	61.6	5.1	8.7
Hyd. 1	0.1	1.2	98.3	21.9	70.7	4.3	1.4
Hyd. 2	0.0	0.9	98.8	22.2	70.9	4.4	1.4
HP 350 °C	0.0	0.0	99.9	28.9	66.6	4.0	0.3
HP 370 °C	0.0	0.1	99.8	33.3	61.3	4.6	0.6
HP 390 °C	0.0	0.3	99.6	37.1	56.1	5.3	1.1

4.8. Gas Composition

During the reactions, a large amount of fully hydrogenated hydrocarbon gas is produced (8–25 wt%, depending on process parameters). Their further use depends on their composition, which is depicted in Figure 17. The relative amount of each component is remarkably similar between PW and FTW cracking, even though the overall amount differs (see Figure 7). Very little methane and almost no ethane is produced. This is due to the fact that the dominant catalytic mechanism would require the presence of primary carbocations, which are highly unstable [21]. The main products are n-propane, n-butane, and iso-butanes. An increase in reactor temperature results in a higher yield of C_3, while the amount of C_4 stays similar, the residual C_{5+} fraction is significantly reduced.
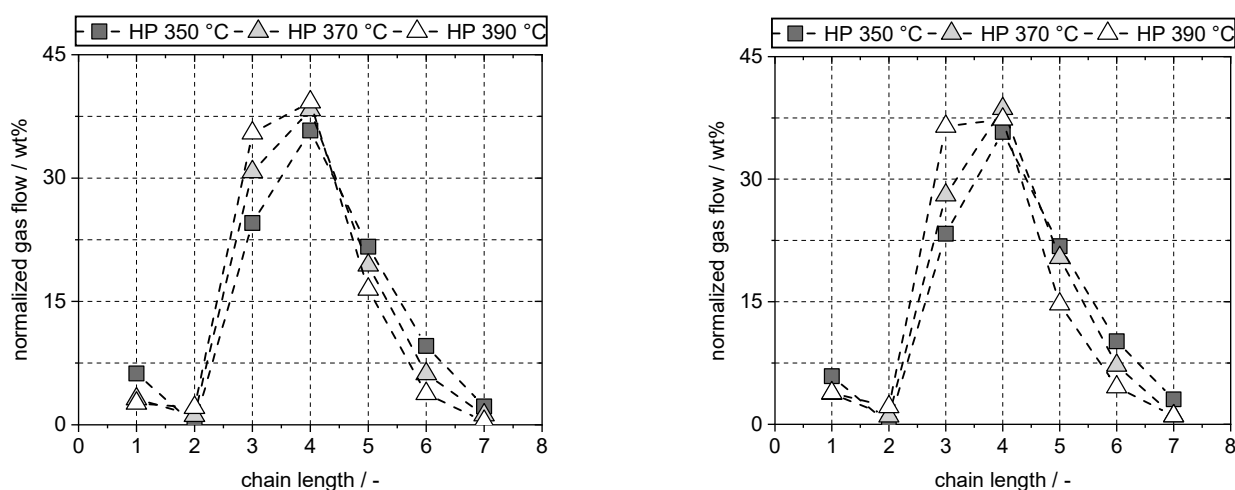
Figure 17. Chain length distribution of hydrocarbon gases produced during hydroprocessing of PW (**left**) and FTW (**right**).

The fraction of isomers for C_{4+} is approximately 45% through all experimental parameters, regardless of feedstock. A detailed summary of the gas phase composition with all the produced isomers listed can be viewed in Table 6. With this information in mind, it is feasible to identify possible use cases for these gases. Due to its similarity to liquified petroleum gas (LPG) [39], it can be used as such. The issue here is that it is not possible to use the gases for fuel in material recycling scenarios. Therefore, the most likely application is recycling into olefins, especially propene, butene, and iso-butenes. This can be done through propane dehydrogenation (PDH), butane dehydrogenation (BDH), or LPG steam cracking [40].

Table 6. Composition of hydrocarbon gases after PW and FT hydroprocessing experiments in relation to the introduced liquid feed.

	PW			FT		
	HP 350 °C	HP 370 °C	HP 390 °C	HP 350 °C	HP 370 °C	HP 390 °C
	(wt%)	(wt%)	(wt%)	(wt%)	(wt%)	(wt%)
Methane	**0.42**	**0.50**	**0.58**	**0.47**	**0.53**	**0.60**
Ethane	**0.00**	**0.18**	**0.47**	**0.00**	**0.14**	**0.33**
Propane	**1.65**	**4.94**	**7.95**	**1.85**	**3.99**	**5.69**
Butanes	**2.41**	**6.15**	**8.80**	**2.84**	**5.49**	**5.83**
n	*1.32*	*3.52*	*4.98*	*1.48*	*3.07*	*3.16*
2-M-Propane	*1.09*	*2.63*	*3.82*	*1.35*	*2.42*	*2.67*
Pentanes	**1.46**	**3.12**	**3.69**	**1.73**	**2.90**	**2.30**
n	0.68	1.49	1.69	0.74	1.29	0.97
2-M-Butane	0.78	1.63	2.00	0.99	1.61	1.33
Hexanes	**0.64**	**0.99**	**0.85**	**0.81**	**1.03**	**0.71**
n	*0.30*	*0.41*	*0.30*	*0.35*	*0.42*	*0.25*
2-M-Pentane	*0.23*	*0.39*	*0.36*	*0.31*	*0.40*	*0.28*
3-M-Pentane	*0.11*	*0.18*	*0.18*	*0.14*	*0.21*	*0.17*
Heptanes	**0.15**	**0.19**	**0.09**	**0.24**	**0.14**	**0.16**
n	*0.11*	*0.07*	*0.02*	*0.13*	*0.08*	*0.08*
2-M-Hexane	*0.01*	*0.04*	*0.02*	*0.01*	*0.01*	*0.01*
3-M-Hexane	*0.04*	*0.08*	*0.04*	*0.10*	*0.05*	*0.06*
Total$_{Gas}$	**6.73**	**16.07**	**22.43**	**7.93**	**14.22**	**15.61**
Total$_{Liquid}$	**92.35**	**83.79**	**75.10**	**92.96**	**87.12**	**83.31**
Total	99.07	99.85	97.53	100.89	101.35	98.91

5. Conclusions

The production of lubricants from real plastic waste was investigated and compared to those produced from Fischer–Tropsch wax. It was shown that it is possible to obtain a high-quality lubricant from polyethylene-based plastic waste through hydrotreatment of the pyrolysis liquids. The produced lubricants from plastic waste showed better temperature stability at identical cloud points than the lubricants from FT waxes. During this research, it was possible to analyze each outgoing product stream towards its further application with a keen focus on potential use in a steam cracker as naphtha substitute. The naphtha phase showed an increasing amount of naphthenes and isomers with rising temperature. To reduce the amount of aromatic components in the naphtha, a noble metal catalyst appears to be necessary. It was possible to compile a complete mass balance from waste to lubricant, which showed potential yields in the range of 13–24 $kg_{Naphtha}$ per 100 $kg_{Plastic\ Waste}$ that could be used as steam cracker substitute. As a high value byproduct, 4–17 kg_{Lube} per 100 $kg_{Plastic\ Waste}$ could also be produced; yields were dependent on process parameters. As an outlook, the approach presented here could be applied to other plastic waste fractions of interest in order to compare high value product yields and to evaluate potential economical and ecological performance.

Conflicts of Interest: The authors declare no conflict of interest.

Appendix A

Table A1. Individual Mass Balances.

Hydrogenation					
	Pyrolysis Wax				
	Hyd. 1 (wt%)			Hyd. 2 (wt%)	
Gas yield	Not determinable			Not determinable	
Liquid yield	100.8			98.7	
Hydroprocessing					
	Pyrolysis Wax			Fischer–Tropsch Wax	
	HP 350 °C (wt%)	HP 370 °C (wt%)	HP 390 °C (wt%)	HP 350 °C (wt%)	HP 370 °C (wt%)	HP 390 °C (wt%)
Gas yield	6.7	16.1	22.4	7.93	14.22	15.61
Liquid yield	92.3	83.8	75.1	92.96	87.12	83.31
Total	99.1	99.9	97.5	100.89	101.34	98.92
Distillation Data					
	Pyrolysis Wax			Fischer–Tropsch Wax	
	HP 350 °C (wt%)	HP 370 °C (wt%)	HP 390 °C (wt%)	HP 350 °C (wt%)	HP 370 °C (wt%)	HP 390 °C (wt%)
Naphtha	21.4	35.2	50.0	5.5	21.7	31.8
Middle distillate	48.6	44.1	33.1	16.1	20.7	27.7
Heavy residue	28.3	18.3	9.0	75.2	52.8	28.5
Distillation loss	1.7	2.4	7.9	3.2	4.7	12.0
Total	100.0	100.0	100.0	100.0	100.0	100.0

Appendix B

Table A2. Tabulated Naphtha Composition.

HP 350 °C (FT)

C_{Number}	4	5	6	7	8	9	10	11	12+	Poly	Total
Naph.	0	0.06	0.75	1.54	1.1	0.29	0.05	0	0	0	**3.78**
i-Par.	0.71	5.45	13.8	16.4	10.01	3.52	1.02	0.15	0.28	0	**51.34**
n-Par.	1.1	6.4	14.95	13.05	6.37	1.98	0.59	0.34	0	0	**44.79**
Cycl Ol.	0	0	0	0	0	0	0	0	0	0	**0**
Olef.	0	0	0.01	0	0	0	0	0	0	0	**0.01**
Arom.	0	0	0	0.03	0	0	0	0	0.04	0	**0.07**
Total	**1.82**	**11.91**	**29.52**	**31.01**	**17.48**	**5.79**	**1.66**	**0.49**	**0.32**	**0**	**100**

HP 370 °C (FT)

	4	5	6	7	8	9	10	11	12+	Poly	Total
Naph.	0	0.11	1.24	1.2	0.31	0.05	0	0	0	0	**2.91**
i-Par.	0.74	7.16	22.59	15.39	3.1	0.58	0.11	0.02	0	0	**49.7**
n-Par.	1.33	9.92	24.87	9.31	1.45	0.29	0.11	0.04	0	0	**47.32**
Cycl Ol.	0	0	0	0	0	0	0	0	0	0	**0**
Olef.	0	0.02	0.04	0.02	0	0	0	0	0	0	**0.07**
Arom.	0	0	0	0.01	0	0	0	0	0	0	**0.01**
Total	**2.07**	**17.21**	**48.74**	**25.93**	**4.85**	**0.91**	**0.23**	**0.06**	**0**	**0**	**100**

HP 390 °C (FT)

	4	5	6	7	8	9	10	11	12+	Poly	Total
Naph.	0	0.1	0.89	1.73	1.5	0.78	0.29	0	0	0.02	**5.31**
i-Par.	0.46	6.96	16.19	15.27	10.32	6.02	3.02	1.05	1.03	0	**60.32**
n-Par.	1.21	8.65	12.43	6.96	2.97	1.1	0.35	0.4	0	0	**34.06**
Cycl Ol.	0	0	0	0	0	0	0	0	0	0	**0.01**
Olef.	0	0.01	0.01	0.01	0.01	0.01	0	0	0	0	**0.05**
Arom.	0	0	0	0.04	0.05	0.03	0	0	0.12	0	**0.25**
Total	**1.67**	**15.71**	**29.51**	**24.03**	**14.85**	**7.94**	**3.66**	**1.45**	**1.15**	**0.02**	**100**

HP 350 °C (PW)

	4	5	6	7	8	9	10	11	12+	Poly	Total
Naph.	0	0.05	1.49	5.05	6.72	5.6	3.11	0.68	0	0.84	**23.54**
i-Par.	0.39	2.17	4.27	5.18	5.48	6.52	3.49	1.82	4	0	**33.33**
n-Par.	0.52	2.79	5.21	6.26	8.74	9.28	6.43	3.1	0	0	**42.34**
Cycl Ol.	0	0	0	0	0	0	0	0	0	0	**0**
Olef.	0	0	0.01	0.01	0	0	0.01	0.01	0	0	**0.05**
Arom.	0	0	0	0.05	0.11	0.05	0	0	0.54	0	**0.75**
Total	**0.91**	**5.02**	**10.98**	**16.55**	**21.06**	**21.45**	**13.04**	**5.61**	**4.55**	**0.84**	**100**

HP 370 °C (PW)

	4	5	6	7	8	9	10	11	12+	Poly	Total
Naph.	0	0.08	1.54	4.32	5.38	4.29	2.15	0.63	0	0.6	**18.98**
i-Par.	0.58	3.81	7.18	7.19	6.95	7.23	4.39	1.73	2.67	0	**41.73**
n-Par.	0.95	5.3	7.72	6.56	6.89	6.06	3.47	1.69	0	0	**38.65**
Cycl Ol.	0	0	0	0	0	0	0	0	0	0	**0**
Olef.	0	0	0.01	0.01	0.01	0	0	0	0	0	**0.04**
Arom.	0	0	0	0.06	0.1	0.1	0	0	0.33	0	**0.6**
Total	**1.53**	**9.19**	**16.44**	**18.14**	**19.34**	**17.68**	**10.01**	**4.06**	**3.01**	**0.6**	**100**

HP 390 °C (PW)

	4	5	6	7	8	9	10	11	12+	Poly	Total
Naph.	0	0.12	1.78	4.29	5.05	4.12	2.13	0.65	0	0.59	**18.73**
i-Par.	0.58	4.85	9.42	8.14	7.6	7.72	5.3	2.48	2.86	0	**48.95**
n-Par.	1.06	6.73	8.54	5.47	4.41	3.07	1.44	0.78	0	0	**31.51**
Cycl Ol.	0	0	0	0	0	0	0	0	0	0	**0**
Olef.	0	0	0	0	0	0	0	0	0	0	**0**

Table A2. *Cont.*

Arom.	0	0	0	0.08	0.14	0.17	0.08	0	0.34	0	**0.81**
Total	**1.63**	**11.7**	**19.75**	**17.98**	**17.21**	**15.08**	**8.94**	**3.91**	**3.2**	**0.59**	**100**
Hyd. 1											
Naph.	0	0.05	1.15	4.06	5.65	5.6	3.97	0.86	0	1.06	**22.41**
i-Par.	0	0	0.17	0.53	1.52	3.81	1.11	1.36	5.07	0	**13.56**
n-Par.	0	0.06	1.32	4.57	10.33	13.96	12.82	5.87	0	0	**48.92**
Cycl Ol.	0	0	0.07	0.6	1.11	0.92	0.4	0.08	0	0	**3.18**
Olef.	0	0	0.1	0.23	0.37	0.94	0.34	0.11	0	0	**2.09**
Arom.	0	0	0	1.89	3.24	3.03	0.86	0	0.81	0	**9.84**
Total	**0**	**0.11**	**2.81**	**11.88**	**22.21**	**28.25**	**19.51**	**8.29**	**5.88**	**1.06**	**100**
Hyd. 2											
Naph.	0	0.06	1.95	5.74	7.98	7.01	4.36	0.84	0	0.89	**28.84**
i-Par.	0	0.01	0.24	0.75	1.93	4.87	1.08	1.2	3.97	0	**14.07**
n-Par.	0	0.09	1.5	4.99	11.26	13.86	11.04	4.6	0	0	**47.33**
Cycl Ol.	0	0	0	0	0	0	0	0.02	0	0	**0.02**
Olef.	0	0	0	0	0	0.01	0	0.02	0	0	**0.03**
Arom.	0	0	0.5	2.07	3.45	2.41	0.57	0	0.7	0	**9.71**
Total	**0**	**0.16**	**4.19**	**13.55**	**24.63**	**28.17**	**17.05**	**6.69**	**4.68**	**0.89**	**100**
Educt											
Naph.	0	0.01	0.2	0.87	1.09	1.41	0.56	0	0	2.65	**6.79**
i-Par.	0	0	0.05	0.05	0.64	0.33	0.15	0.49	4.67	0	**6.37**
n-Par.	0.07	0.11	0.23	1.37	2.83	3.02	2.06	1.1	0	0	**10.78**
Cycl Ol.	0	0.06	1.27	3.25	3.84	3.15	1.36	0.56	0	0	**13.49**
Olef.	0.04	0.27	1.95	4.88	9.85	16.21	10.05	3.68	0	0	**46.93**
Arom.	0	0	0.77	3.06	7.25	2.91	0.68	0	0.96	0	**15.64**
Total	**0.11**	**0.45**	**4.47**	**13.47**	**25.49**	**27.02**	**14.88**	**5.83**	**5.63**	**2.65**	**100**

Appendix C

Table A3. Viscosity Measurements of FT and PW Lubricants at Constant Sher Rate 50 s^{-1}.

	Viscosity FT_{Lube} (mm^2/s)			Viscosity PW_{Lube} (mm^2/s)		
	20 °C	40 °C	100 °C	20 °C	40 °C	100 °C
HP 350 °C	-	23.34	5.62	111.20	18.08	4.61
HP 370 °C	49.05	22.93	5.17	40.11	18.80	4.55
HP 390 °C	32.41	15.20	3.60	21.36	12.54	3.30

References

1. Dahmen, N.; Dinjus, E.; Kolb, T.; Arnold, U.; Leibold, H.; Stahl, R. State of the art of the bioliq® process for synthetic biofuels production. *Environ. Prog. Sustain. Energy* **2012**, *31*, 176–181. [CrossRef]
2. Müller, S.; Groß, P.; Rauch, R.; Zweiler, R.; Aichernig, C.; Fuchs, M.; Hofbauer, H. Production of diesel from biomass and wind power—Energy storage by the use of the Fischer-Tropsch process. *Biomass Convers. Biorefin.* **2018**, *8*, 275–282. [CrossRef]
3. Royal Dutch Shell plc. Risella X High-Quality Technical White Oils Based on Gas to Liquids (GTL) Technology. Available online: https://go.shell.com/2RnueBW (accessed on 4 May 2021).
4. Statista. Benzinpreis. Zusammensetzung im März 2022. Available online: https://de.statista.com/statistik/daten/studie/29999/umfrage/zusammensetzung-des-benzinpreises-aus-steuern-und-kosten/ (accessed on 21 April 2022).
5. Ritchie, H.; Roser, M. Plastic Pollution. 2018. Available online: https://ourworldindata.org/plastic-pollution (accessed on 17 May 2022).
6. Hauli, L.; Wijaya, K.; Syoufian, A. Hydrocracking of LDPE Plastic Waste into Liquid Fuel over Sulfated Zirconia from a Commercial Zirconia Nanopowder. *Orient. J. Chem.* **2019**, *35*, 128–133. [CrossRef]

7. Kunwar, B.; Cheng, H.N.; Chandrashekaran, S.R.; Sharma, B.K. Plastics to fuel. A review. *Renew. Sustain. Energy Rev.* **2016**, *54*, 421–428. [CrossRef]

8. Choi, I.-H.; Lee, H.-J.; Rhim, G.-B.; Chun, D.-H.; Lee, K.-H.; Hwang, K.-R. Catalytic hydrocracking of heavy wax from pyrolysis of plastic wastes using Pd/Hβ for naphtha-ranged hydrocarbon production. *J. Anal. Appl. Pyrolysis* **2022**, *161*, 105424. [CrossRef]

9. Miller, S.J.; Chevron U.S.A. Inc. Process for Converting Waste Plastic into Lubricating Oils. U.S. Patent 6,822,126 B2, 23 November 2004. Available online: https://patents.google.com/patent/US6822126B2/en (accessed on 5 July 2022).

10. Miller, S.J.; Shah, N.; Huffman, G.P. Conversion of Waste Plastic to Lubricating Base Oil. *Energy Fuels* **2005**, *19*, 1580–1586. [CrossRef]

11. Kusenberg, M.; Eschenbacher, A.; Djokic, M.R.; Zayoud, A.; Ragaert, K.; Meester, S.; de van Geem, K.M. Opportunities and challenges for the application of post-consumer plastic waste pyrolysis oils as steam cracker feedstocks. To decontaminate or not to decontaminate? *Waste Manag.* **2022**, *138*, 83–115. [CrossRef]

12. Galperin, L.N. Hydroisomerization of N-decane in the presence of sulfur and nitrogen compounds. *Appl. Catal. A Gen.* **2001**, *209*, 257–268. [CrossRef]

13. Kobayashi, M.; Ishida, K.; Saito, M.; Yachi, H.; Japan Energy Corporation. Lubricant Base Oil Method of Producing the Same. U.S. Patent 8.012,342 B2, 6 September 2011. Available online: https://bit.ly/3phwTtk (accessed on 5 July 2022).

14. Kobayashi, M.; Saitoh, M.; Togawa, S.; Ishida, K. Branching Structure of Diesel and Lubricant Base Oils Prepared by Isomerization/Hydrocracking of Fischer−Tropsch Waxes and α-Olefins. *Energy Fuels* **2009**, *23*, 513–518. [CrossRef]

15. Karaba, A.; Rozhon, J.; Patera, J.; Hájek, J.; Zámostný, P. Fischer-Tropsch Wax from Renewable Resources as an Excellent Feedstock for the Steam-Cracking Process. *Chem. Eng. Technol.* **2021**, *44*, 329–338. [CrossRef]

16. Wang, F.; Xu, Y.; Ren, J.; Li, Y. Experimental investigation and modeling of steam cracking of Fischer–Tropsch naphtha for light olefins. *Chem. Eng. Process. Process Intensif.* **2010**, *49*, 51–58. [CrossRef]

17. Hsu, C.S.; Robinson, P.R. *Petroleum Science and Technology*; Springer Nature: Cham, Switzerland, 2019; ISBN 978-3-030-16275-7. [CrossRef]

18. Passut, C.; Barton, P.; Klaus, E.; Tewksbury, E. Low-Temperature Ketone Dewaxing of Mineral Oils by Direct Cooling. *Ind. Eng. Chem. Res.* **1977**, *16*, 120–124. [CrossRef]

19. Taylor, R.J.; McCormack, A.J. Study of solvent and catalytic lube oil dewaxing by analysis of feedstocks and products. *Ind. Eng. Chem. Res.* **1992**, *31*, 1731–1738. [CrossRef]

20. Cody, I.A. Selective Hydroprocessing for new lubricant standards. In *Practical Advances in Petroleum Processing*; Hsu, C.S., Robinson, P.R., Eds.; Springer: New York, NY, USA, 2006. [CrossRef]

21. Bouchy, C.; Hastoy, G.; Guillon, E.; Martens, J.A. Fischer-Tropsch Waxes Upgrading via Hydrocracking and Selective Hydroisomerization. *Oil Gas Sci. Technol. Rev. L'ifp* **2009**, *64*, 91–112. [CrossRef]

22. Pichler, H.; Schulz, H.; Reitemeyer, H.O.; Weitkamp, J. Über das Hydrokracken gesättigter Kohlenwasserstoffe. *Erdöl Und Kohle Erdgas Petrochem. Ver. Mit Brennst. Chem.* **1972**, *25*, 494–505.

23. Tulloch, A.P. The composition of beeswax and other waxes secreted by insects. *Lipids* **1970**, *5*, 247–258. [CrossRef]

24. Nuissier, G.; Bourgeois, P.; Grignon-Dubois, M.; Pardon, P.; Lescure, M.H. Composition of sugarcane waxes in rum factory wastes. *Phytochemistry* **2002**, *61*, 721–726. [CrossRef]

25. de Klerk, A. *Catalysis in the Refining of Fischer-Tropsch Syncrude*; RSC Publishing: Cambridge, UK, 2010; ISBN 978-8-84973-080-8.

26. Zeller, M.; Netsch, N.; Richter, F.; Leibold, H.; Stapf, D. Chemical Recycling of Mixed Plastic Wastes by Pyrolysis—Pilot Scale Investigations. *Chem. Ing. Tech.* **2021**, *93*, 1763–1770. [CrossRef]

27. Neuner, P.; Graf, D.; Mild, H.; Rauch, R. Catalytic Hydroisomerisation of Fischer–Tropsch Waxes to Lubricating Oil and Investigation of the Correlation between Its Physical Properties and the Chemical Composition of the Corresponding Fuel Fractions. *Energies* **2021**, *14*, 4202. [CrossRef]

28. Deldari, H. Suitable catalysts for hydroisomerization of long-chain normal paraffins. *Appl. Catal. A Gen.* **2005**, *293*, 1–10. [CrossRef]

29. Lee, S.-W.; Ihm, S.-K. Hydroisomerization and hydrocracking over platinum loaded ZSM-23 catalysts in the presence of sulfur and nitrogen compounds for the dewaxing of diesel fuel. *Fuel* **2014**, *134*, 237–243. [CrossRef]

30. Brunet, S.; Mey, D.; Pérot, G.; Bouchy, C.; Diehl, F. On the hydrodesulfurization of FCC gasoline. A review. *Appl. Catal. A Gen.* **2005**, *278*, 143–172. [CrossRef]

31. Mochida, I.; Choi, K.-H. An Overview of Hydrodesulfurization and Hydrogenation. *J. Jpn. Pet. Inst.* **2004**, *47*, 145–163. [CrossRef]

32. *ASTM D2500-17a*; Test Method for Cloud Point of Petroleum Products and Liquid Fuels. ASTM International: West Conshohocken, PA, USA, 2018. [CrossRef]

33. Claudy, P.; Letoffe, J.-M.; Neff, B.; Damin, B. Diesel fuels: Determination of onset crystallization temperature, pour point and filter plugging point by differential scanning calorimetry. Correlation with standard test methods. *Fuel* **1986**, *65*, 861–864. [CrossRef]

34. Europäisches Arzneibuch. *Amtliche Deutsche Ausgabe*; Deutscher Apotheker Verlag: Stuttgart, Germany, 2017; ISBN 9783769266412.

35. *ASTM D2502-14*; Test Method for Estimation of Mean Relative Molecular Mass of Petroleum Oils from Viscosity Measurements. ASTM International: West Conshohocken, PA, USA, 2020. [CrossRef]

36. Bruycker, R.; de Amghizar, I.; Vermeire, F.H.; Nyman, T.; Hakola, M.; van Geem, K.M. Steam cracking of bio-derived normal and branched alkanes. Influence of branching on product distribution and formation of aromatics. *J. Anal. Appl. Pyrolysis* **2016**, *122*, 468–478. [CrossRef]

37. Kopinke, F.D.; Zimmermann, G.; Reyniers, G.C.; Froment, G.F. Relative rates of coke formation from hydrocarbons in steam cracking of naphtha. 2. Paraffins, naphthenes, mono-, di-, and cycloolefins, and acetylenes. *Ind. Eng. Chem. Res.* **1993**, *32*, 56–61. [CrossRef]

38. Kusenberg, M.; Roosen, M.; Zayoud, A.; Djokic, M.R.; Dao Thi, H.; Meester, S.; de Ragaert, K.; Kresovic, U.; van Geem, K.M. Assessing the feasibility of chemical recycling via steam cracking of untreated plastic waste pyrolysis oils. Feedstock impurities, product yields and coke formation. *Waste Manag.* **2022**, *141*, 104–114. [CrossRef]

39. Mylpg.eu. LPG Propane/Butane Mixture. Available online: https://www.mylpg.eu/de/nutzliche-info/autogasgemisch/ (accessed on 21 April 2022).

40. Bender, M. An Overview of Industrial Processes for the Production of Olefins—C 4 Hydrocarbons. *ChemBioEng Rev.* **2014**, *1*, 136–147. [CrossRef]